Inflow-Sensitive Inversion Recovery SSFP Imaging of the Carotid Arteries: A Potential Strategy for Noncontrast MRA of the Neck

P. Young[1], M-M. Khalighi[2], A. Brau[3], N. Takei[4], W. Sun[5], and R. Herfkens[6]

[1]Radiology, Stanford University, Stanford, California, United States, [2]Applied Science Laboratory West, GE Healthcare, Menlo Park, California, United States, [3]Applied Science Laboratory West, GE Healthcare, Menlo Park, California, [4]Applied Science Laboratory Japan, GE Healthcare, Tokyo, Japan, [5]MR Engineering, GE Healthcare, Waukesha, Wisconsin, United States, [6]Radiology, Stanford University, Palo Alto, California, United States

Introduction: Carotid and vertebral MRA is commonly performed and typically employs gadolinium contrast agents. A significant limitation to the technique occurs in patients for whom gadolinium contrast is contra-indicated. While time-of-flight (TOF) techniques can be employed to obtain reasonably good noncontrast MR images of these arteries, the quality of such images rarely matches that of contrast-enhanced exams. Steady-state free precession (SSFP) imaging can provide "bright-blood" contrast while avoiding some of the spin saturation seen under low-flow states in time of flight applications (1), although high background signal can be problematic. We describe our initial experience imaging the carotid and vertebral arteries using an inflow-sensitive SSFP sequence which was initially developed for imaging of the renal arteries (2,3).

Methods and Materials: Studies were conducted using an investigational version of GE's Inhance Inflow IR (IFIR) pulse sequence. This uses a spatially selective inversion pulse covering the area to be imaged as well as the area distal to it in order to suppress venous inflow. This is followed with a respiratory triggered axial SSFP readout with chemical fat suppression.

9 healthy volunteers (6 M, 3F, age 27-32) underwent imaging (resulting in 18 carotid and 18 vertebral arteries for analysis). Volunteers were positioned with their heads in an 8 channel cardiac coil in a 1.5T GE Signa magnet. Typical imaging parameters were TR 4.5, TE 2.3, Flip angle 70, TI 1300ms, Matrix 256x256 , FOV 35 , Slice thickness 2mm, # locs 80, Pixel BW 488Hz. ASSET parallel imaging was used to increase the speed of image acquisition. Total scan time was typically 5 minutes. The craniocaudal distance over which the common and internal carotid and vertebral arteries could be reasonably assessed was measured, and the number of external carotid artery branches which could be visualized over at least 2 cm was recorded. Images were also assessed for adequacy of background suppression and poorly suppressed areas were noted.

Results: The average length of carotid artery visualization in our volunteer population was 12.3 +/- 3.0 cm, with a range of 8.8-15.5 cm. The average vertebral artery length covered was 10.6 +/- 2.7 cm, with a range of 6.1-14.3 cm. In most volunteers, signal in the internal carotid arteries was lost once they entered the petrous segment. The average number of external carotid arterial branches seen was 5.7 +/- 1.3. In all but one volunteer, 6 or 7 of the 8 typical external carotid artery branches were visualized. In 5 of 9 volunteers, some fat suppression was lost in the shoulders and chin; these areas were all either at the edge of the imaging field or very close to the coil. In 4 of 9 volunteers, signal in the CSF was incompletely suppressed. While in none of the cases would this likely have presented a diagnostic dilemma on interpretation of axial images, the signal did make processing of maximum intensity projection and volume rendered images more difficult.

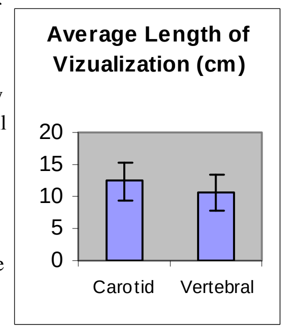

Conclusion: In our volunteers, the length reliably imaged in an acquisition was such that anatomical coverage could be extended from the aortic arch to the carotid bifurcation or from the bifurcation to the skull base, but not from the arch to the skull base. The limited coverage and variability that exists between patients presumably varies according to the rate of carotid inflow and the selected inversion time. Clinical use of this technique would likely require at least two acquisitions to cover the extent of the carotid and vertebral arteries. In addition, the diminished inflow which would likely occur in many clinical patients (from arterial stenosis or diminished cardiac output) might further limit the area which could be imaged in a single acquisition. Additional work also remains to be done in ascertaining the relative merits of this technique versus TOF and contrast-enhanced MRA under varying flow states. The lost background suppression seen in some of our volunteers would probably be improved by optimizing inversion time, and the poor fat suppression sometimes seen was probably because we used a cardiac coil rather than a neurovascular coil. However, the preliminary results are promising and worthy of further investigation and optimization.

Figures:

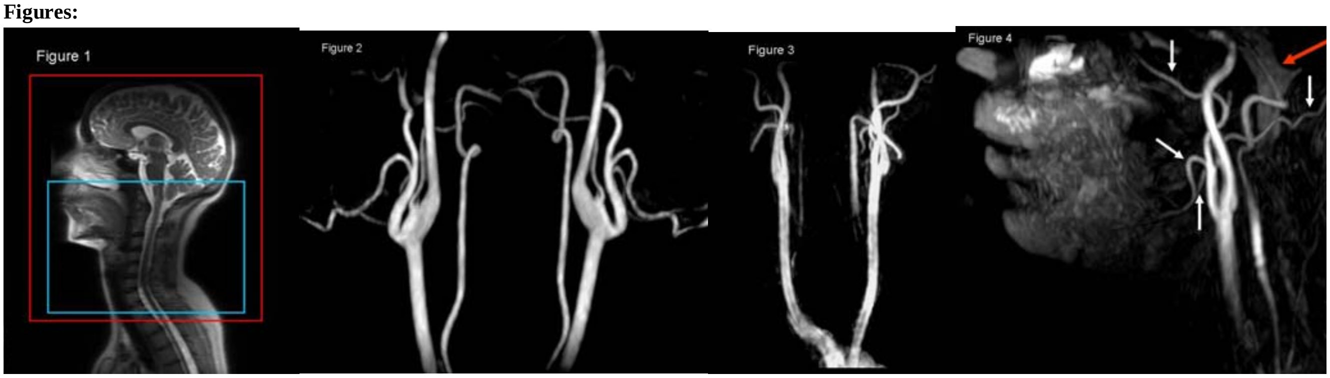

Figure 1: Schematic depicting the relationship of the inversion pulse (red rectangle) and imaging area (blue rectangle), on the scout image

Figure 2: . Coronal maximum intensity projection (MIP) reconstruction of IFIR images of the carotid and vertebral arteries demonstrates good visualization of the common, internal, and external carotid arteries as well as the vertebral arteries from the lower neck through the skull base.

Figure 3: Coronal MIP with coverage greatly extended to the aortic arch. Note that visualization of the distal extracranial internal carotid arteries is inadequate since inflow has not reached the skull base by the time of image acquisition.

Figure 4: Lateral oblique MIP demonstrates larger branches of the external carotid artery (white arrows). Note supboptimal suppression of signal in the subject's face near the coil, as well as in the CSF (red arrow).

References:

1. Fuchs F et al. Eur J Radiol 2003; 46:28-32. 2. Nishimura D. et al., MRM 1988; 7 :472-484. 3. Takei N. et al., Proceedings of ISMRM, 3420 (2008).